Adaptive Filters for Color Images: Median Filtering and Its Extensions

Andreas Kleefeld[1], Michael Breuß[1(✉)], Martin Welk[3], and Bernhard Burgeth[2]

[1] Faculty of Mathematics, Natural Sciences and Computer Science, Brandenburg Technical University Cottbus-Senftenberg, 03046 Cottbus, Germany
{kleefeld,breuss}@tu-cottbus.de
[2] Department of Mathematics and Computer Science, Saarland University, 66123 Saarbrücken, Germany
burgeth@math.uni-sb.de
[3] Biomedical Image Analysis Division, Department of Biomedical Computer Science and Mechatronics, University for Medical Informatics and Technology (UMIT), Eduard-Wallnöfer-Zentrum 1, 6060 Hall/Tyrol, Austria
martin.welk@umit.at

Abstract. In this paper we are concerned with robust structure-preserving denoising filters for color images. We build on a recently proposed transformation from the RGB color space to the space of symmetric 2×2 matrices that has already been used to transfer morphological dilation and erosion concepts from matrix-valued data to color images. We investigate the applicability of this framework to the construction of color-valued median filters. Additionally, we introduce spatial adaptivity into our approach by morphological amoebas that offer excellent capabilities for structure-preserving filtering. Furthermore, we define color-valued amoeba M-smoothers as a generalization of the median-based concepts. Our experiments confirm that all these methods work well with color images. They demonstrate the potential of our approach to define color processing tools based on matrix field techniques.

Keywords: Matrix field · Color image · Median filter · M-smoother · Amoeba filter

1 Introduction

Thanks to modern technology, digital color images have become a ubiquitous element of our every-day life, creating an ever-increasing demand for efficient algorithms to process color image data. With noise being one of the most widespread sources of image degradation, denoising is a crucial task of image processing. Despite decades of research, it continues to pose new challenges, not least due to the ongoing spread of imaging into new application fields with unfavorable acquisition conditions with higher noise levels and an increasing diversity of noise sources. For example, low-light photography by mobile phones combined with

© Springer International Publishing Switzerland 2015
A. Trémeau et al. (Eds.): CCIW 2015, LNCS 9016, pp. 149–158, 2015.
DOI: 10.1007/978-3-319-15979-9_15

compression for low-rate data transfer may lead to mixtures of significant sensor noise with scattered light and compression noise. To cope with such application contexts requires robust and structure-preserving denoising approaches. Whereas the present work does not aim at giving a fully developed algorithm for a specific application problem, it intends to contribute to the development of robust denoising algorithms. Our approach combines a suitable choice of color space with multi-channel median filtering on adaptive neighborhoods. The median filter component is later generalized by so-called M-smoothers. In the following, we therefore provide some background on these four concepts.

Color Spaces. Since the output of most digital image sensors consists of red, green, and blue intensity values, the corresponding RGB color space is often used to perform color image processing. Targeting at the enhancement of images for human observers, it makes sense, however, to adopt a color space that reflects better the sensitivity and contrast perception of the human visual system. In the latter, the excitations of retina cones, which are close to an RGB model, undergo several transformation steps before they become color impressions, giving rise to several color spaces that relate to different steps in this chain. From this realm, the hue-chroma-luminance (HCL) lends itself as a good compromise for image denoising because it is on one hand close enough to the RGB input and thereby to the physical noise process, whilst at the same time it reflects reasonably the perceptual metric of human color vision.

Color image processing is embedded in the context of multi-channel image processing, which includes e.g. processing of tensor fields [11] as well. An interesting link between the concepts developed there and color image processing results from the structure of the HCL, HSV and similar color spaces. The latter model the gamut of colors as a cone or bi-cone with a luminance or brightness value as axial dimension. Likewise, symmetric positive definite matrices as are used to represent diffusion tensors form a cone whose axial dimension represents an overall intensity. In [4] this relation has been fruitfully exploited to transfer multi-channel morphology concepts from tensor data to color image processing.

Median Filtering. For gray-scale images, a time-proven method for robust denoising is median filtering [10], which establishes a filtered image by assigning to each pixel the median of gray values from the input image within a neighborhood of that pixel. Neighborhoods for all pixels are generated by shifting a fixed-shape mask across the image. The process can be iterated, by computing a first filtered image from the input, a second filtered image from the first one, and so on. This procedure can cope with heavy-tailed noise distributions such as salt-and-pepper noise, whilst preserving important image features like edges that are crucial for human interpretation of images.

Attempts to transfer median filtering to multi-channel contexts like color images have therefore been made as early as 1990 [2]. The notion of vector median introduced there selects as median of a finite set of vectors always one of the input vectors. While this is advantageous in terms of algorithmic complexity, it leads to discontinuous dependence of output data from input data, and applied

to color images, to noticeable color artifacts, as demonstrated in [8]. Indeed, a median concept that drops the restriction to select one of the input values has already been proposed several decades before by Weiszfeld [12]. Following these, the median of data points in a metric space is the point in the same space that minimizes the sum of distances to the input values. This notion of median has been applied to color images in [8] via the RGB color space. The same approach has been introduced to tensor field processing in [15].

Adaptive Neighborhoods. For each pixel, the median filtering procedure involves two steps: a sliding-window *selection* step, and the *aggregation* of selected input values via the median. To increase the sensitivity to important image structures, the selection step can be modified by using spatially adaptive neighborhoods. One representative of these are *morphological amoebas* as introduced by Lerallut et al. [5], see also the further analysis in [13,14]. In this approach, spatial distance in the image plane is combined with contrast into an image-adaptive metric. On the basis of this metric, adaptive neighborhoods called amoebas are established and used to replace the sliding window in median filtering in order to perform adaptive filtering.

M-Smoothers. Combining the sliding-window selection step with different aggregation operators leads to other well-known image filters, such as average filter (with aggregation by mean value), morphological dilation and erosion (with maximum or minimum). A general class of position estimators for univariate distributions are M-estimators, which include median and mean value as special cases [7]. In combination with the sliding-window procedure they give rise to image filters called *M-smoothers* [9].

Our Contributions. In this paper, we combine the ideas reviewed in the preceding paragraphs in several ways. First, we use the color-tensor link from [4] to transfer the median filtering idea of [15] to color images and compare the resulting version of a color median filter with the RGB-based approach from [8]. This is further combined with the amoeba approach [5] for spatial adaptive filtering to yield a color amoeba median filter with enhanced structure preservation. Second, we transfer the tensor-valued M-smoothers studied in [15] to color images and combine them with the amoeba approach.

2 Color Images and Matrix Fields

In this section, we briefly recall the conversion of RGB-images to matrix fields as introduced in [4]. Given an RGB-image we transform it in two steps into a matrix field $\mathbf{F}$ of equal dimensions, i.e. we assign each pixel of the image a symmetric 2×2 matrix.

In the first step, we transform the color values of the image from the RGB representation to the HCL color space. We assume that red, green and blue intensities are normalized to $[0, 1]$. For a pixel with red, green and blue intensities r, g, b, resp., we obtain its hue h, chroma c and luminance l via $M = \max\{r, g, b\}$, $m = \min\{r, g, b\}$, $c = M - m$, $l = \frac{1}{2}(M + m)$, and $h = \frac{1}{6}(g - b)/M$ modulo 1 if

$M = r$, $h = \frac{1}{6}(b-r)/M + \frac{1}{3}$ if $M = g$, $h = \frac{1}{6}(r-g)/M + \frac{2}{3}$ if $M = b$, compare [1, Algorithm 8.6.3]. Replacing further the luminance l with $\tilde{l} := 2l - 1$, and interpreting c, $2\pi h$, and $\tilde{l}$ as radial, angular and axial coordinates, resp., of a cylindrical coordinate system, we have so far a bijection from the unit cube of triples (r, g, b) onto a solid bi-cone, see Figure 1. Its base is the unit disc in the plane $\tilde{l} = 0$, while its tips correspond to $\tilde{l} = \pm 1$ on the $\tilde{l}$-axis. The bi-cone is then transformed from cylindrical to Cartesian coordinates via $x = c\cos(2\pi h)$, $y = c\sin(2\pi h)$, $z = \tilde{l}$.

The second step takes the Cartesian coordinate triples (x, y, z) and maps them to symmetric matrices $A \in \mathrm{Sym}(2)$ via

$$A = \frac{\sqrt{2}}{2}\begin{pmatrix} z-y & x \\ x & z+y \end{pmatrix}, \qquad (1)$$

compare [4]. Note that the mapping $\Psi : \mathbb{R}^3 \to \mathrm{Sym}(2)$ defined by (1) is bijective and even an isometry from the Euclidean space $\mathbb{R}^3$ to the space Sym(2) with the metric defined by the Frobenius norm $\|\cdot\|_{\mathrm{F}}$, $d(A, B) := \|A - B\|_{\mathrm{F}}$. Denoting by $\mathcal{M} \subset \mathrm{Sym}(2)$ the set of all matrices A which correspond to points of the bi-cone, we have therefore a bijection between the RGB color space and the bi-cone $\mathcal{M}$ in Sym(2). The inverse transform from matrices to RGB triples is obtained in a straightforward way, compare [4].

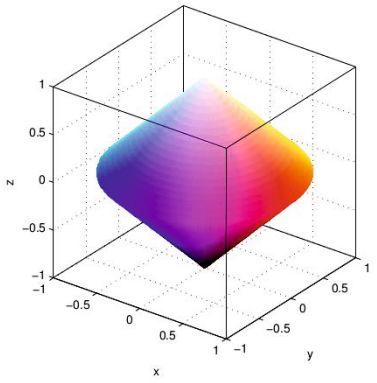

Fig. 1. Color bi-cone, figure adapted from [3]

To illustrate the conversion of color values, we state RGB, Cartesian bi-cone and symmetric matrix representations of exemplary colors in Table 1.

3 Constructing Amoebas

In this section, we explain how to construct an adaptive, pixel-wise varying filtering domain, *amoeba* for short, for a given matrix field $\mathbf{F}$. In doing this we

Table 1. Colors and their RGB, Cartesian bi-cone and matrix representations

Color	Black	Red	Green	Blue
(r, g, b)	$(0, 0, 0)$	$(1, 0, 0)$	$(0, 1, 0)$	$(0, 0, 1)$
(x, y, z)	$(0, 0, -1)$	$(1, 0, 0)$	$(-1/2, \sqrt{3}/2, 0)$	$(-1/2, -\sqrt{3}/2, 0)$
A	$-\frac{\sqrt{2}}{2}\begin{pmatrix} 1 & 0 \\ 0 & 1 \end{pmatrix}$	$\frac{\sqrt{2}}{2}\begin{pmatrix} 0 & 1 \\ 1 & 0 \end{pmatrix}$	$-\frac{1}{4}\begin{pmatrix} \sqrt{6} & \sqrt{2} \\ \sqrt{2} & -\sqrt{6} \end{pmatrix}$	$-\frac{1}{4}\begin{pmatrix} -\sqrt{6} & \sqrt{2} \\ \sqrt{2} & \sqrt{6} \end{pmatrix}$
Color	Yellow	Magenta	Cyan	White
(r, g, b)	$(1, 1, 0)$	$(1, 0, 1)$	$(0, 1, 1)$	$(1, 1, 1)$
(x, y, z)	$(1/2, \sqrt{3}/2, 0)$	$(1/2, -\sqrt{3}/2, 0)$	$(-1, 0, 0)$	$(0, 0, 1)$
A	$\frac{1}{4}\begin{pmatrix} -\sqrt{6} & \sqrt{2} \\ \sqrt{2} & \sqrt{6} \end{pmatrix}$	$\frac{1}{4}\begin{pmatrix} \sqrt{6} & \sqrt{2} \\ \sqrt{2} & -\sqrt{6} \end{pmatrix}$	$-\frac{\sqrt{2}}{2}\begin{pmatrix} 0 & 1 \\ 1 & 0 \end{pmatrix}$	$\frac{\sqrt{2}}{2}\begin{pmatrix} 1 & 0 \\ 0 & 1 \end{pmatrix}$

extend the approach of Lerallut et al. in a straightforward fashion: In [5], color channels have been considered separately for amoeba construction.

Let (x_i, y_i) be the coordinates of the i-th pixel of an image with gray-value f_i. For a given pixel i_0 with coordinates (x_{i_0}, y_{i_0}) the amoeba is constructed as follows. As a first step, we only consider pixels i^* that are located in a prescribed maximal Euclidean distance ϱ of pixel i_0 which limits the maximal size of the amoeba. As a second step, we take these pre-selected pixels and consider paths $(i_0, i_1, \ldots, i_k \equiv i^*)$ which connect i_0 with i^* allowing only pixels that are neighbors to enter P. We determine the *shortest path* P among all those possibilies using the *amoeba distance* $L(P)$, a combination of spatial and tonal distances, defined by

$$L(P) = \sum_{m=0}^{k-1} 1 + \sigma \sum_{m=0}^{k-1} \left| f_{i_{m+1}} - f_{i_m} \right| , \tag{2}$$

where $\sigma > 0$ is a given parameter that penalizes large deviations in gray-valued data. If $L(P) \leq \varrho$ for P holds, then pixel i^* is a member of the amoeba.

Because the amoeba distance includes a tonal distance, the amoeba has the ability to grow around structures given by large tonal differences, compare the sketches in Figure 2: A filter applied over fixed masks takes into account all values as e.g. here both white and gray region, while an amoeba may grow around corners as indicated.

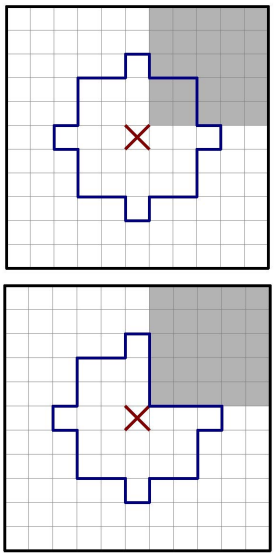

Fig. 2. Masks centered at marked pixels. **Top.** Spatially fixed window. **Bottom.** Amoeba domain.

Note that modifications of this approach are possible and have been done by Welk et al. [14]. Precisely, they considered 8-point instead of 4-point neighbors as we do in this work, and different distance measures. To efficiently implement the amoeba computation we use the fast marching method similarly as in [13,14].

Since we deal with matrix fields, we have to consider an amoeba distance defined for matrices. A natural extension of (2) is

$$L(P) = \sum_{m=0}^{k-1} 1 + \sigma \sum_{m=0}^{k-1} \left\| F_{i_{m+1}} - F_{i_m} \right\|_{\mathrm{F}} \tag{3}$$

where F_i is the symmetric matrix of size 2×2 at the coordinate (x_i, y_i). Here, $\|\cdot\|_F$ denotes the Frobenius norm, which we employ in all computations. Of course, also other norms like e.g. the nuclear norm [6, p. 615] are possible, however, one should not employ different norm definitions for amoeba distance and the filtering methods described in the following.

4 Median Filtering and Its Generalizations

Given a color image, we first convert it to a matrix field as described in Section 2. Then amoebas are constructed via the procedure given in Section 3 for all pixels.

For an amoeba as an adaptive structuring element, it is possible to extract the matrices $A_1, \ldots, A_n$ that participate in it.

Median Filters. The Frobenius matrix median M of this set of symmetric 2×2 matrices is given by

$$M := \mathrm{med}_{\mathrm{F}}(A_1, \ldots, A_n) := \arg\min_{X \in \mathrm{Sym}(2)} \sum_{i=1}^{n} \|X - A_i\|_{\mathrm{F}} \tag{4}$$

compare for example [15]. Note that the matrices $A_1, \ldots, A_n$ represent points in a solid bi-cone defining a convex set. The resulting median is located in the convex hull of this set and hence, the median operation never leads to RGB color values outside the unit cube, see [15, Proposition 2]). To calculate the median numerically one may reformulate the problem as a convex minimization problem; compare [15, Section3.2.1] for the reformulation and a discussion.

Given a matrix field $\mathbf{F}^{(0)} := \mathbf{F}$, an amoeba median filter works now as follows. For each matrix in the matrix field, one computes the amoeba, selects the set of matrices $A_1, \ldots, A_n$, and computes the Frobenius matrix median. The resulting matrix is stored in the matrix field $\mathbf{F}^{(1)}$.

An *iterated amoeba median filter* (IAMF) applies this procedure iteratively p times yielding matrix fields $\mathbf{F}^{(0)}, \ldots, \mathbf{F}^{(p)}$. At the end, the resulting matrix field $\mathbf{F}^{(p)}$ is converted back to a RGB image. In the subsequent section we report the experimental results when this procedure is applied to various color test images.

M-Smoothers. Next, we consider a generalization of the median filter that can be traced back to Barral Souto [7] by modifying (4) as

$$M_p := \arg\min_{X \in \mathrm{Sym}(2)} \sum_{i=1}^{n} \|X - A_i\|_{\mathrm{F}}^{p} \tag{5}$$

where we assume $p \geq 1$ to ensure uniqueness of the minimizer, cf. [13, pp.20–21]). The symmetric matrix M_p is called a *matrix-valued M-smoother*. For $p = 1$ we recover the median, for $p = 2$ we obtain the arithmetic mean, and for the limiting case $p \to \infty$ the mid-range. Using amoebas and calculating the M-estimators iteratively leads to an *iterated amoeba M-smoothers* (IAMS).

5 Experiments

The structure of our experimental section is as follows. First we confirm that the use of our new color scheme for both amoeba construction and filtering gives better results than simpler amoeba-based methods employed in a similar style as by Lerallut et al. [5] where experiments were designed to give a proof of concept. Then we show an experiment demonstrating benefits of amoeba structuring elements over fixed filtering masks. This is followed by a comparison of our new set-up for median filtering with a recent method for median computation working with RGB data, namely the method of Spence and Fancourt [8]. Finally, we present some results of our new amoeba-based M-smoothers.

Comparison with a Simple Amoeba-Based Median Filter. The purpose of this experiment is to demonstrate that the use of amoebas alone without a proper median computation cannot give high-quality results.

To this end we take up a test image used in [5], see Figure 3. The image in the middle is obtained by a simple, amoeba-based iterated median filtering. Here the median is determined channel-wise in RGB, iterating three times amoeba construction and median filtering analogously to IAMF. This is compared with three iterations IAMF by our method, see the image on the right hand side.

Fig. 3. IAMF versus amoeba-based simple median computation, amoeba parameters are $\varrho = 5$ and $\sigma = 5$. **Left.** Input image, size 131×173. **Middle.** Result for amoebas and channel-wise median filter. **Right.** Result of IAMF with three iterations.

Our method yields reasonable colors after filtering, while the simple channel-based median exhibits the expected problems of color distortions, e.g. have a look at the left part of the nose or at green spots around the eyes and at the transition of hat to background. Let us also note that the expected edge-preserving properties of the amoebas are clearly observable when using a proper median as performed by our method.

Comparison of Amoebas with Fixed Filtering Masks. The purpose of this experiment is to verify that the edge-preserving properties of median amoeba filters that can be observed for gray-valued images [5,13] are carried over to filtering of color images. Because of the well-known difficulties in dealing with color vectors we do not expect that this is self-evident.

In order to illuminate the mentioned effect we employ a low resolution test image of size 64×64, see Figure 4. In the first row we demonstrate the edge-preserving capability of the amoebas and show that our color scheme for median filtering gives reasonable results. The shape of the peppers is well-preserved while regions of similar color are more uniform after IAMF, in contrast to plain median filtering which shows expected rounding effects of image structures. By the second row we demonstrate that our method is capable of delivering reasonable shape information if the input is perturbed by noise. Note that the stipe

Fig. 4. Amoebas versus fixed filtering mask with iterated median filter. **Left column.** Input images, original (top) and with added Gaussian noise in each channel (bottom). **Middle column.** Iterated median filtering with our color scheme for 3×3 masks and three iterations. **Right column.** IAMF with $\sigma = 5$, $\varrho = 3$ and three iterations.

of the thin pepper is not well preserved in the filtering process. The filtering of this kind of thin, oblique structures can be improved by using 8-neighborhoods instead of 4-neighborhoods in the amoeba construction; however, we leave this algorithmical improvement to future research. Note also that we employed $\varrho = 3$ in this test instead of $\varrho = 5$ in Fig. 3, since the resolution of the input image in Fig. 4 is much lower and the parameter ϱ controls the maximal size of the structuring element.

Comparison to RGB-Based Color Median Approach. The aim of this experiment is to show that our median filter based on our specific color representation yields competitive results compared to a RGB-based method for median filtering, namely the approach of Spence and Fancourt [8].

The Figure 5 shows results for the *Hamburg* test image. We filter the image with IAMF with parameters $\varrho = 5$, $\sigma = 5$ and perform three iterations. Let us note that in order to achieve directly comparable results, we adjust the parameter σ by the factor $\sqrt{4/3}$ when using the method of Spence and Fancourt. This factor can be derived by considering the distances between black and white in RGB space and our color space, respectively. As can be expected from the similarity of the methods, the results of our approach and that from [8] are largely comparable.

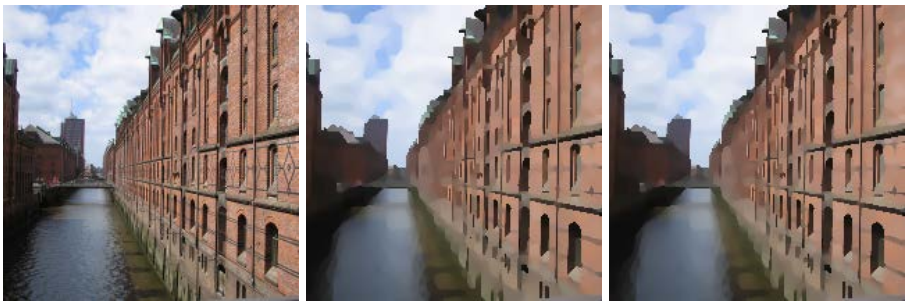

Fig. 5. Comparison of IAMF with 5 iterations, $\varrho = 5$, $\sigma = 5$, for different color median filters. **Left.** Input image, size 213×213. **Middle.** Method of Spence and Fancourt. **Right.** Our color scheme.

Iterated Amoeba M-Smoothers. For demonstrating the flexibility of our framework we present in Figure 6 results for IAMS with several values for p, see (5). The results show that image simplification can be achieved by our method without color distortions. Results with fixed structuring elements are equally possible but not very illustrative here. We observe the expected increased smoothing effect when letting p grow combined with the edge-preserving mechanism of the amoebas.

Fig. 6. Matrix-valued M-smoothers with exponent p and 5 iterations. **Left.** IAMS with $p = 1$ identical to IAMF. **Middle.** IAMS with $p = 2$, i.e. the image shows an amoeba-based arithmetic mean. **Right column.** IAMS with $p = 5$.

6 Conclusion

In this paper we have extended the work from [3] on using matrix fields for the processing of color images. We have introduced a color median filter concept based on this approach and used it in connection with morphological amoebas for robust, structure-preserving image denoising. We have also formulated a

more general filter class of color amoeba M-smoothers. Our experiments demonstrate the viability and versatility of the approach. Ongoing work is directed at generalizations to further image filters and applications for color image processing. For future work we aim to make our algorithm more efficient and to exploit theoretical connections of our approach to bilateral filtering and related concepts.

References

1. Agoston, M.K.: Computer Graphics and Geometric Modeling: Implementation and Algorithms. Springer, London (2005)
2. Astola, J., Haavisto, P., Neuvo, Y.: Vector median filters. Proceedings of the IEEE **78**(4), 678–689 (1990)
3. Burgeth, B., Kleefeld, A.: An approach to color-morphology based on Einstein addition and Loewner order. Pattern Recognition Letters **47**, 29–39 (2014)
4. Burgeth, B., Kleefeld, A.: Order based morphology for color images via matrix fields. In: Burgeth, B., Vilanova, A., Westin, C.-F. (eds.) Visualization and Processing of Tensor Fields and Higher Order Descriptors for Multi-Valued Data. Springer, Berlin (2014)
5. Lerallut, R., Decencière, E., Meyer, F.: Image processing using morphological amoebas. In: Ronse, C., Najman, L., Decencière, E. (eds.) Mathematical Morphology: 40 Years On Computational Imaging and Vision, vol. 30, pp. 13–22. Springer, Dordrecht (2005)
6. Schatten, R., von Neumann, J.: The cross-space of linear transformations. II. Annals of Mathematics **47**(3), 608–630 (1946)
7. Souto, J.B.: El modo y otras medias, casos particulares de una misma expresión matemática. Technical Report 3, Cuadernos de Trabajo, Instituto de Biometría, Universidad Nacional de Buenos Aires, Argentina (1938)
8. Spence, C., Fancourt, C.L.: An iterative method for vector median filtering. In: Proceedings of the International Conference on Image Processing, ICIP 2007, San Antonio, Texas, USA, September 16–19, pp. 265–268 (2007)
9. Torroba, P.L., Cap, N.L., Rabal, H.J., Furlan, W.D.: Fractional order mean in image processing. Optical Engineering **33**(2), 528–534 (1994)
10. Tukey, J.W.: Exploratory Data Analysis. Addison-Wesley, Menlo Park (1971)
11. Weickert, J., Hagen, H. (eds.): Visualization and Processing of Tensor Fields. Springer, Berlin (2006)
12. Weiszfeld, E.: Sur le point pour lequel la somme des distances de n points donnés est minimum. Tôhoku Mathematics Journal **43**, 355–386 (1937)
13. Welk, M., Breuß, M.: Morphological amoebas and partial differential equations. In: Hawkes, P. (ed.) Advances in Imaging and Electron Physics, vol. 185, pp. 139–212. Academic Press, Elsevier Inc. (2014)
14. Welk, M., Breuß, M., Vogel, O.: Morphological amoebas are self-snakes. Journal of Mathematical Imaging and Vision **39**, 87–99 (2011)
15. Welk, M., Weickert, J., Becker, F., Schnörr, C., Feddern, C., Burgeth, B.: Median and related local filters for tensor-valued images. Signal Processing **87**, 291–308 (2007)